MODELING AND ANALYSIS OF INTERNAL THREAD FORMING

Sameer Chowdhary, O. Burak Ozdoganlar, Shiv G. Kapoor, Richard E. DeVor
Department of Mechanical and Industrial Engineering
University of Illinois at Urbana-Champaign, Urbana, IL 61801, USA

ABSTRACT

This paper presents a mechanistic model for the prediction of thrust and torque experienced by a forming tap during an internal thread forming process. The model relates the forces to the area of contact between the tool and the workpiece. Experiments are conducted to calibrate and validate the model. The model-predicted thrust and torque values compare favorably with the experimental values. Sensitivity analysis was conducted to examine the effect of relief and entry taper angles on the forces generated during the process.

INTRODUCTION

Thread forming is being increasingly employed by industry because of the higher productivity rates and the elimination of chips. Unfortunately, relatively little is known about the mechanics of the thread forming process. The ability to predict the forces generated during thread forming process will be helpful in designing better taps and in the selection of the tapping conditions that lead to optimal results.

Most of the attempts to model the thread forming process to date have focussed on the external thread forming using rolling dies [5, 6, 21]. Hayama [12] developed a model, using the minimum energy method and the partially plastic deformed thick walled cylinder theory to predict the maximum torque values experienced during the internal thread forming process. Henderer and von Turkovich [13, 14] developed a theoretical model to predict the final torque in form tapping using slip line field theory. The model predicted the sensitivity of torque to a number of tapping parameters such as tap size, hole size, entry taper angle, degree of bluntness of the teeth on the entry taper and the concentric thread flank contact area. Ivanov and Kirov [16, 17] developed an empirical formula for finding the maximum value of torque experienced in internal thread forming. They also concluded that it is possible to roll internal threads with forming taps in both ferrous and non-ferrous metals provided that their brinell hardness and tensile strength are not above 200 and 800 Mpa, respectively.

In a form tapping operation, each tooth on the entry taper of the tap acts as a forming tool. As each tooth on the entry taper comes into contact with the workpiece, it deforms the workpiece material in front of it. This deformed material flows upwards along the faces of the tooth and is deposited on the sides of the grooves formed by the tooth. This deposition is known as a ridge. These ridges increase in height as more and more material from the grooves flows out with each successive tooth deforming the workpiece to greater depths, and ultimately assume the shape of the crests of the final thread form.

The forces developed during the process are both due to the deformation of the workpiece material and the resulting flow of the deformed material along the faces of the tooth [12]. Since there is always an elastic portion beneath the plastically deformed material that tries to recover once the forces causing the material to deform are removed, there will be an increase in the forces experienced during the process. Plastic deformation will also result in the work hardening of the workpiece material. Thus, the two major factors contributing to the forces during a forming process are the deformation of the material by the tool and the elastic recovery of the material.

Any comprehensive model for the form tapping process should be able to capture both these phenomena.

To date, the models developed for internal thread forming predict only the final torque value and thrust predictions have been conspicuous by their absence. This paper focuses only on the modeling of deformation of the workpiece and the resulting flow of the material along the faces of the tool on the torque and thrust forces with the aim of predicting both the instantaneous torque and instantaneous thrust experienced during the internal thread forming process.

Experiments at the tooth-level using two axially-consecutive teeth are discussed first. The understanding thus obtained is applied to develop a mechanistic model. The model relates the forces developed during the process to the area of contact between the tool and the workpiece through specific forming energies. A calibration methodology is presented for the evaluation of the specific forming energies through experiments. Results obtained from the model validation are also presented. Effects of variation in parameters of the tap on the forces generated during the process are examined.

TOOTH-LEVEL EXPERIMENTS

To simplify the analysis of the internal thread forming process, the initial focus was on the mechanisms at the tooth level, i.e., the determination of the nature of forces experienced by a single tooth as it deforms the workpiece material. To develop an appropriate tool for this purpose, all but two axially-consecutive teeth on a form tap were removed to capture the forces developed due to the flow of deformed material in between these teeth.

The dotted lines in Figure 1 represent the longitudinal and cross-sectional views of a form tap and the solid lines represent the tool used for the tooth-level experiments. d_{min} and d_{max} are the radial distances of the crests of the teeth with minimum and maximum height from the center of the tap. The entry taper and the back taper angles, two of the important angles that define the tap geometry, are also shown in the figure. The entry taper is provided to distribute the total deformation to be done amongst several teeth and the back taper angle minimizes the contact area of the other teeth with the workpiece, thereby reducing the frictional forces. H is the hole radius. The lube grooves, seen on the cross-section of the tap, are provided on the tap body to facilitate the flow of coolant and/or lubricant to the portions of the tap involved in forming.

The experiments at tooth level were done on Mori-Seiki SH-400 Horizontal Machining Center. Orthogonal motion, as opposed to rotary motion, was used for the tooth-level experiments because of the concerns about runout, uncertainty in the depth of cut due to the difficulty in obtaining the exact hole diameter and tooth breakage. The forces developed during the process were collected using a 4-component Kistler dynamometer Model No. 9272. The experiments were done at

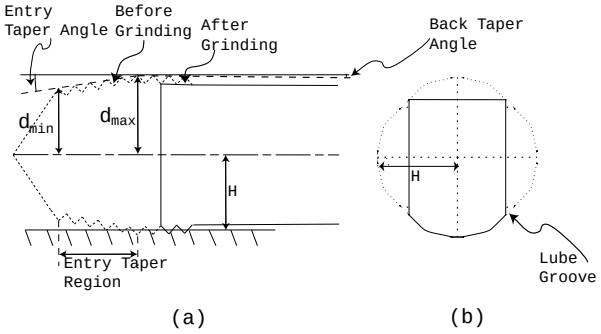

FIGURE 1: (a) FORM TAP; (b) CROSS-SECTION OF A FORM TAP.

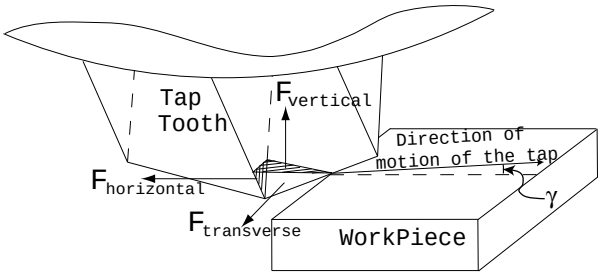

FIGURE 2: A SINGLE TAP TOOTH.

surface speeds ranging from 10 m/min to 20 m/min and depths of cut ranging from 0.05 mm to 0.40 mm (approximately equal to the depth of cut for the teeth on the entry taper). A M10 X 1.5 tap and brass were used as the tool and workpiece, respectively. The lubricant used was Microsol 265. To maintain orthogonal contact, the tool was moved on the workpiece at an angle equal to the lead angle (γ = 2.73 degrees) of the tap as shown in Figure 2. The experimental setup is shown in Figure 3.

Figures 4 and 5 show the force signals generated during several of the tooth-level experiments. It is evident from these figures that the forces are developed in all three (horizontal, vertical and transverse) directions. This indicates that the tooth is non-symmetric about the lead direction, i.e., the direction of motion. These experiments also confirmed that the forces remain constant during the traversal of a tooth on the workpiece at a constant depth of cut. Figures 4 and 5 also reveal that increasing either the speed or the depth of cut increases the forces experienced by the tool.

MODELING

Model Assumptions

The assumptions made for the model development are as follows:

- The workpiece material does not stick to the tap

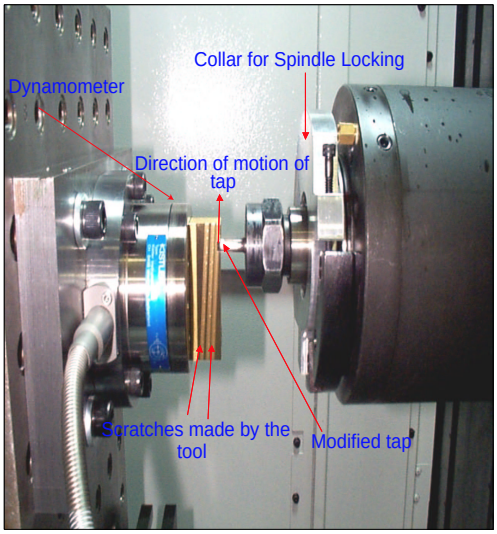

FIGURE 3: THE EXPERIMENTAL SETUP FOR TOOTH-LEVEL EXPERIMENTS.

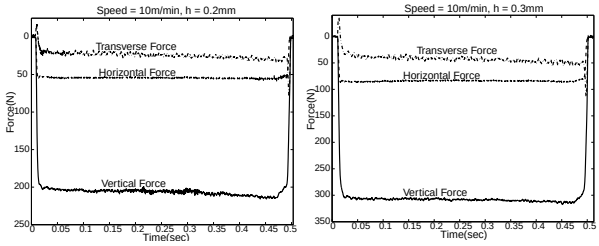

FIGURE 4: THE FORCES AT h = 0.2 mm AND h = 0.3 mm FOR 10 m/min SURFACE SPEED.

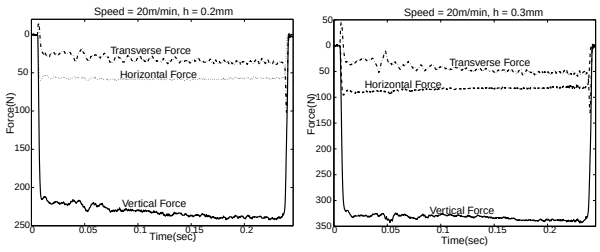

FIGURE 5: THE FORCES AT h = 0.2 mm AND h = 0.3 mm FOR 20 m/min SURFACE SPEED.

tooth after deformation, i.e., the adhesion forces between the workpiece and the tool material are negligible;

- The effect of elastic recovery is not accounted for in this model. This model considers the effect of the deformation forces only;
- The forces experienced due to the deformation caused by one tooth will remain constant throughout the process;
- These forces are assumed to be proportional to the area of contact between the tooth and the workpiece. These proportionality constants, like the specific cutting energies are assumed to follow the power law;
- The flow of the deformed material along the tooth faces follows Stabler's rule, i.e., the material flow angle along a face is equal to the inclination angle of that face from the perpendicular to the direction of motion;
- Each face of the tap tooth is assumed to be experiencing a normal force and a frictional force that act at the centroid of the respective faces.

Model Development

The isometric view of Figure 6 shows the material flow angle, η_l, which is the angle between the frictional force, F_{fl}, and the perpendicular to the edge 43. There will be a similar angle, η_t, on the trailing face of the tooth between the frictional force, F_{ft}, and the perpendicular to the edge 42. In the side view, the depth of engagement of the tooth, h, in the workpiece can be seen. The top view shows the y-component of distance between point 1 and point 4, p, and the y-component and z-component of distance between point 4 and point 3 or point 2, q and v, respectively. α is called the thread angle of the given thread form, and β is the relief angle of the tooth.

The normal force, F_n, and frictional force, F_f, on each face are assumed proportional to the area of contact between that face and the workpiece.

Thus, the forces on the i^{th} tooth are given as:

$$\begin{aligned} F_{nt}(i) &= C_n(i)A_t(i) \\ F_{nl}(i) &= C_n(i)A_l(i) \\ F_{ft}(i) &= C_f(i)A_t(i) \\ F_{fl}(i) &= C_f(i)A_l(i) \end{aligned} \tag{1}$$

where the $A(i)'s$ represent the areas of the faces of the tooth in contact with the workpiece when viewed along the direction of motion of the tooth and the subscripts t and l represent the trailing and leading faces, respectively. The C(i)'s represent the proportionality constants henceforth called the specific forming energies.

It was seen from the tooth-level experiments that the forces during internal thread forming are dependent on

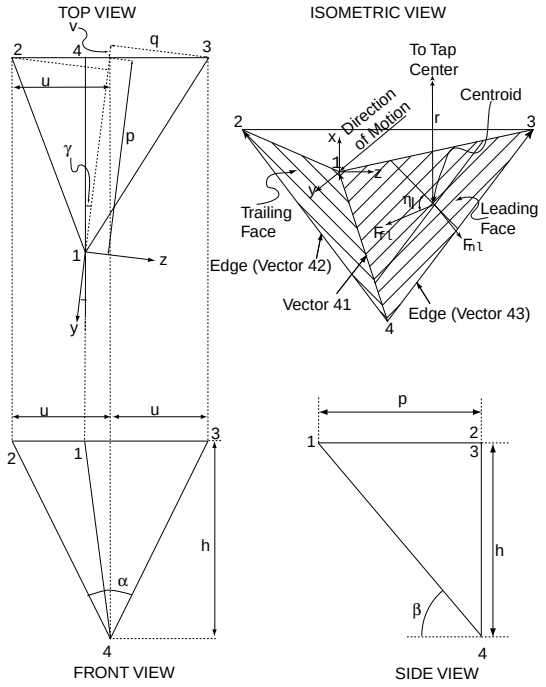

FIGURE 6: GEOMETRY OF A SINGLE TAP TOOTH.

the surface speed of the tool on the workpiece and the depth of cut. Thus, the specific forming energies were assumed to depend on these parameters. Since the present model is based on principles similar to an oblique cutting model where the specific cutting energies, K_n and K_f, follow the power law [4], it was assumed that the specific forming energies can be represented using the same law. Thus, the specific forming energies can be determined from the relations,

$$\begin{aligned} \ln C_n(i) &= a1 + a2 \ln h(i) \ln S(i) + a3 \ln h(i) \\ &\quad + a4 \ln S(i) \\ \ln C_f(i) &= b1 + b2 \ln h(i) \ln S(i) + b3 \ln h(i) \\ &\quad + b4 \ln S(i) \end{aligned} \tag{2}$$

where the a's and b's are determined from calibration experiments for a given tool-workpiece combination and S(i) is the surface speed of the i^{th} tooth and is given as,

$$S(i) = (2 \times N_s \times (h(i) + H))/60 \tag{3}$$

where N_s is the spindle speed in rpm. $h(i)$ is the depth of engagement of the i^{th} tooth with the workpiece. If the total number of the teeth on the entry taper are K, then h(i) is given by,

$$\begin{aligned} &h(i) = d(i) - H, \;\; if \;\; d(i) > H \\ &h(i) = 0, \;\; if \;\; d(i) \leq H \\ &d(i) = d_{min} + (i-1)\triangle d \\ &\triangle d = (d_{max} - d_{min})/K. \end{aligned} \tag{4}$$

The area shaded by single hatching in Figure 7 shows the areas of contact between the trailing and leading tooth faces and the workpiece. These areas are given by,

$$\begin{aligned} A_l(i) &= B_l(i) - B_l(i-1) \\ A_t(i) &= B_t(i) - B_t(i-1) \end{aligned} \tag{5}$$

where the $B(i)'s$ give the total area of the tooth shown by the cross-hatched region in Figure 7. These areas are

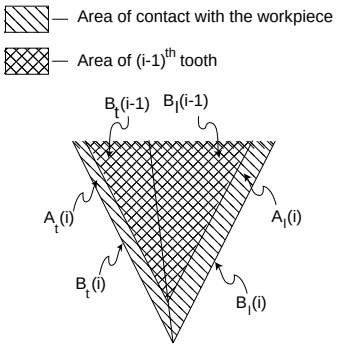

FIGURE 7: THE AREAS OF CONTACT OF THE i^{th} TOOTH.

given as,

$$\begin{aligned} B_l(i) &= |\overrightarrow{43} \times \overrightarrow{41}| \\ &= -p(i)q(i)\hat{x} + h(i)q(i)\hat{y} \\ &\quad + h(i)(p(i) + v(i))\hat{z} \\ B_t(i) &= |\overrightarrow{41} \times \overrightarrow{42}| \\ &= -p(i)q(i)\hat{x} + h(i)q(i)\hat{y} \\ &\quad - h(i)(p(i) - v(i))\hat{z} \end{aligned} \tag{6}$$

where $\hat{x}$, $\hat{y}$, and $\hat{z}$ are the unit vectors in the x, y, and z directions, respectively. $p(i)$, $q(i)$, and $r(i)$ may be evaluated from Figure 6 as follows,

$$\begin{aligned} &p(i) = h(i)/\tan\beta \\ &q(i) = u\cos\gamma \\ &v(i) = u\sin\gamma \\ &u(i) = h(i)\tan(\alpha/2). \end{aligned} \tag{7}$$

The normal and frictional forces can subsequently be transformed into the x,y, and z axes defined in Figure 6 by using transformation equations as given by,

$$\begin{aligned} F_x &= (\vec{F}_{fl} + \vec{F}_{nl} + \vec{F}_{ft} + \vec{F}_{nt}) \cdot \hat{x} \\ F_y &= (\vec{F}_{fl} + \vec{F}_{nl} + \vec{F}_{ft} + \vec{F}_{nt}) \cdot \hat{y} \\ F_z &= (\vec{F}_{fl} + \vec{F}_{nl} + \vec{F}_{ft} + \vec{F}_{nt}) \cdot \hat{z}. \end{aligned} \tag{8}$$

These forces are then transformed into tap coordinates using the following equations (refer to Fig. 8),

$$\begin{aligned} F_{thr} &= F_y \sin\gamma + F_z \cos\gamma \\ F_{tan} &= F_y \cos\gamma - F_z \sin\gamma \end{aligned} \tag{9}$$

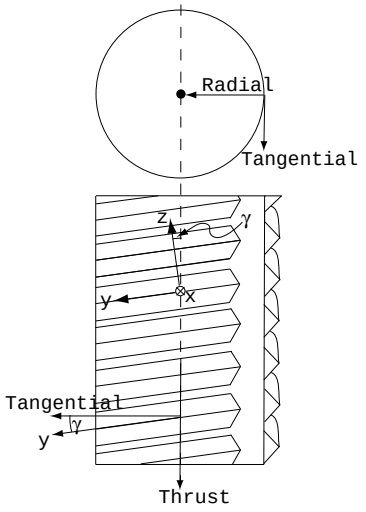

FIGURE 8: TRANSFORMATIONS FROM TOOTH TO TAP COORDINATES.

where F_{thr} and F_{tan} are the forces in the thrust and tangential directions, respectively. The torque, M, on the tooth during forming can be determined by taking the product of the force in the tangential direction, F_{tan}, with r, the radial distance of centroid of the tooth from the center of tap,

$$M = F_{tan} \times r. \tag{10}$$

MODEL CALIBRATION AND VALIDATION

For the purpose of calibrating and validating the model, a set of form tapping experiments was run. The machine used for this purpose was Mori-Seiki TV-30 vertical milling, drilling and tapping machine. The conditions used for the experiments are given in Table 1. A 4-component Kistler dynamometer Model No. 9272 was used to collect the force signals. The holes were reamed before tapping to minimize the effect of hole quality variations on the force signals obtained during the process.

TABLE 1: EXPERIMENTAL CONDITIONS FOR MODEL CALIBRATION AND VALIDATION EXPERIMENTS.

Parameter	Values
Tap Size	M10 × 1.5
Workpiece Material	Brass
Hole Diameter Before Reaming	9.03 mm
Hole Diameter After Reaming	9.347 mm (65% thread)
Speeds	250,500,750,1000 rpm
Coolant	Microsol 265
Thread Angle (α)	60 deg
Relief Angle (β)	75 deg

Calibration Methodology

To find the dependence of the specific forming energies on the depth of engagement $h(i)$, the values of specific forming energies with varying $h(i)$ must be determined. If the normal and frictional forces on each tooth of the tap are known, the specific forming energies can be determined using Equation 1, given the area of contact of each tooth. As the teeth successively come into contact with the workpiece at fixed time intervals, it is possible to isolate the individual contribution of the i^{th} tooth by subtracting the forces observed at the time of engagement of $(i-1)^{th}$ tooth from the forces observed at the time of engagement of i^{th} tooth.

Let t_{i+1} be the time at which the i^{th} tooth comes into contact with the workpiece. Then, the time for which the i^{th} tooth is in contact with the workpiece before the $(i+1)^{th}$ tooth comes into contact is given by:

$$t = t_{i+1} - t_i. \tag{11}$$

Since the tap rotates with a constant speed, N_s, t can be considered to be the same for all the teeth on the tap. t can be determined by using

$$t = 60/(N \times N_s) \tag{12}$$

where N is the number of lube grooves on the tap as shown in Figure 1. t_1 is given by the time at which we see the first non-zero force signal. Once t and t_1 are known, all t_i can be evaluated using Equation 11. Only the first tooth is in contact with the workpiece during time t_1 to t_2, and hence the force signals acquired during this time span are solely due to the interaction between the first tooth and the workpiece. Similarly, from time t_2 to time t_3 first two teeth are the ones in contact with the workpiece and since we already know the contribution of the first tooth, the contribution of the second tooth can be determined.

Once the torque and thrust contributions of all the teeth are determined based on the calibration experiments, the specific forming energies C_n and C_f can be determined for each tooth using Equations 1, 8, and 9. The relations for specific forming energies are found by applying the least squares method to Equation 2 for the calibration experiments conducted at speeds of 250 and 1000 rpm and the other conditions of Table 1. The application of statistical tests of significance for the coefficients yielded the following model:

$$\begin{aligned} lnC_n(i) &= 10.292 - 0.826 \ln h(i) \\ lnC_f(i) &= 11.651 - 0.841 \ln h(i). \end{aligned} \tag{13}$$

Figure 9 shows a comparison of the experimental data and Equation 13 for a speed of 250 rpm.

Model Validation

Model validation experiments were conducted at speeds of 500 and 750 rpm and the other conditions of Table 1.

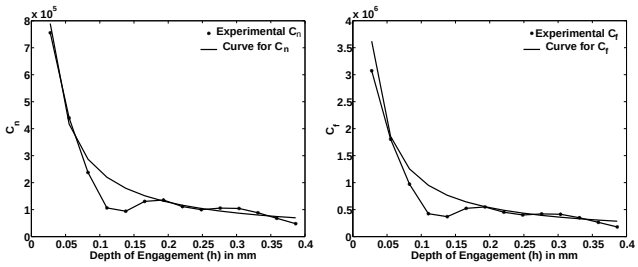

FIGURE 9: THE VARIATION OF C_n AND C_f WITH $h(i)$ AT 250 RPM.

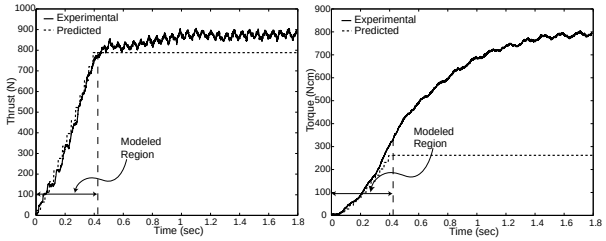

FIGURE 10: PREDICTED AND EXPERIMENTAL VALUES OF THRUST AND TORQUE AT 500 RPM.

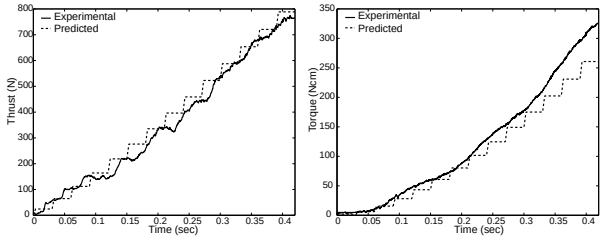

FIGURE 11: PREDICTED AND EXPERIMENTAL VALUES OF THRUST AND TORQUE IN THE MODELED REGION AT 500 RPM.

The predicted and the experimental forces for the whole of the tap entry phase are shown in Figures 10, 11, and 12. The modeled region is that phase of the process in which only the teeth on the entry taper of the tap are in contact with the workpiece. Since elastic recovery has not been accounted for in this model, the teeth on the back taper are not involved in the forming process and thus they do not contribute to the forces. The average percent errors for the thrust and torque values in the modeled region are 8% and 24%, respectively. As can be observed from the Figures 11 and 12, both the experimental and the predicted forces show an expected stair-step pattern, since from the tooth-level experiments it was seen that the forces for a single tooth remain constant throughout the process and thus in the time between the two consecutive teeth coming into contact with the workpiece, the overall forces also should remain constant.

It is observed from Figures 11 and 12 that the predicted torque values do not match up too well with the experimental torque values beyond the modeled region. Once the entry taper of the form tap reaches full engagement (approximately 0.4 sec for the conditions of Figures 10 and 11, and 0.3 sec for the conditions of Figure 12) the model predicts the torque and thrust to be constant, whereas the experimental torque value continues to increase considerably. This discrepancy is likely attributed to elastic recovery.

To predict the total forces incurred in internal thread forming, a model for the effect of elastic recovery also needs to be developed. The forces from the tap exit phase may prove fruitful for obtaining an insight into this problem. Through experimentation it was observed that during the tap exit phase the thrust and torque forces for form tapping do not go to zero as shown in Figure 13. The presence of these forces during the tap exit phase is an indication of the presence of elastic recovery. It is also noted in examining Figures 10 - 13 that unlike cut tapping, the thrust force is very large in form tapping.

EFFECT OF TAP GEOMETRY ON DEFORMATION THRUST AND TORQUE

The model developed above was used to study the effect of changes in the deformation thrust and torque with the changes in some of the process parameters. This helped in corroborating the validity of the model and also in quantitatively assessing the effect of changes in the tap geometry on thrust and torque. The parameters studied were the relief angle and the entry taper angle of the tap.

Effect of Relief Angle

The relief angle of the taps used in this study was measured to be 75 degrees. To study the effect of relief angle, a tap with 76 degrees relief angle was also considered in the analysis. Simulations were conducted for each of these relief angle values for a M10 X 1.5 tap for brass workpieces. The hole diameter selected was 9.347 (65% thread) and the spindle speed was 750 rpm.

Figure 14 shows that the estimated torque is acutely sensitive to changes in relief angle. Both the torque and thrust values increase with increasing relief angle, but the increase in torque is much greater as compared to increase in thrust. Thus, the relief angle should be chosen and controlled carefully.

Effect of Entry Taper Angle

To study the effect of entry taper angle of the tap on the deformation forces experienced during the process, 4 and 6 degree entry taper angles were compared. Simulations were conducted for M10 X 1.5 tap with brass workpieces. The hole diameter selected was 9.347 (65% thread) and the spindle speed used for the simulations was 750 rpm.

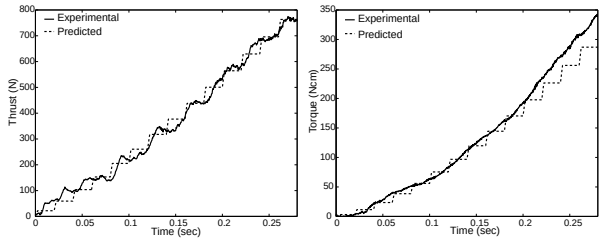

FIGURE 12: PREDICTED AND EXPERIMENTAL VALUES OF THRUST AND TORQUE IN THE MODELED REGION AT 750 RPM.

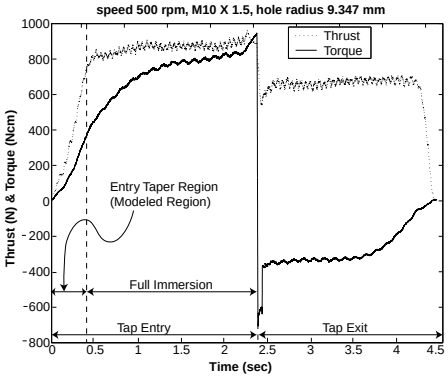

FIGURE 13: EXPERIMENTAL FORCES DURING A TYPICAL FORM TAPPING OPERATION.

Figure 15 shows that the final estimated torque and thrust values remain almost the same inspite of the change in entry taper angle. The number of teeth on the entry taper in contact with the workpiece, though, decreases with increasing entry taper angle, so each tooth engaged sees a larger depth of engagement, $h(i)$. Thus, increasing the entry taper angle does not affect the final values of torque and thrust, but it does increase the individual contribution of each teeth in contact with the workpiece. These increased forces on some of the teeth may lead to an increase in the wear of these teeth and hence may be detrimental to tap life.

CONCLUSIONS

The conclusions that can be drawn from the above work are as follows:

- Tooth-level experiments showed that the forces remain constant during the traversal of a tooth on a workpiece and showed that the form tapping forces are dependent on the surface speed of the tooth on the workpiece and the depth of engagement of the tooth with the workpiece.
- A model for the deformation process was developed wherein the normal and the frictional forces on a tooth are proportional to the area of contact of that tooth with the workpiece. The proportionality constants known as the specific forming energies were assumed to be dependent on the depth of engagement of the tooth and the surface speed of the tooth.
- A calibration procedure was devised to quantify the dependency of the specific forming energies on the depth of engagement and surface speed of teeth on the workpiece, and these dependencies were found to follow the power law, analogous to the specific cutting energies for the case of cut tapping.
- Calibration and validation experiments were conducted on brass with spindle speeds varying from 250-1000 rpm and predicted thrust was found to be in close agreement with the experimental data for the modeled region, which is the region when only the teeth on the entry taper are in contact with the workpiece. It was observed that both the experimental and the predicted force signals show a stair-step pattern.
- The predicted torque values were found to be consistently lower than the experimental values in the modeled region. This discrepancy may be attributed to the presence of elastic recovery.
- The model simulations revealed that varying the entry taper angle does not affect the final values of the forces, though larger entry taper angles might prove to be detrimental for the tap life. It was also seen that increasing the relief angle increases torque forces significantly.

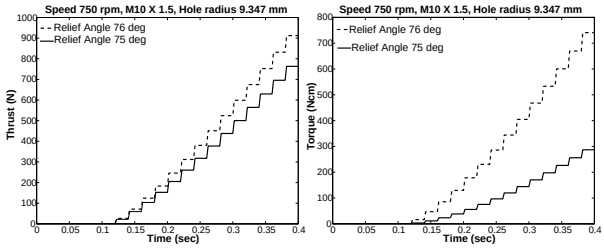

FIGURE 14: PREDICTED THRUST AND TORQUE VALUES FOR DIFFERENT RELIEF ANGLES.

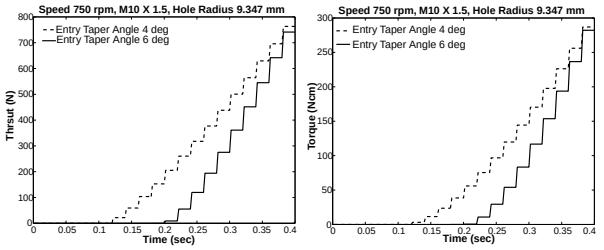

FIGURE 15: PREDICTED THRUST AND TORQUE VALUES FOR DIFFERENT ENTRY TAPER ANGLES.

ACKNOWLEDGEMENT

The authors gratefully acknowledge the support of the National Science Foundation and the UIUC Center for Machine-Tool Systems Research. The authors would also like to thank Dr. Ted Henderer of Kennametal for his valuable input and suggestions.

REFERENCES

[1] Agapiou, J. S., (1994), "Evaluation of the effect of high speed machining on tapping," ASME Transactions, Journal of Engineering for Industry, Vol. 116, pp. 457-462.

[2] Bowden, F. P. and D. Tabor, (1966), "Friction, lubrication and wear: A survey of work during the last decade," British Journal of Applied Physics, Vol. 17, pp. 1521-1544.

[3] Childs, T. H. C., (1970), "The sliding of rigid cones over metals in high adhesion conditions," International Journal of Mechanical Sciences, Vol. 12, pp. 393-403.

[4] Dogra, A. S., S. G. Kapoor, and R. E. DeVor, (1999), "Mechanistic model for tapping process with emphasis on process faults and hole geometry," ASME, Manufacturing Engineering Division, Vol. 10, pp. 271-283.

[5] Domblesky, J. P., (1999), "Computer simulation of thread rolling processes," Fastener Technology International, No. 8, pp. 38-40.

[6] Domblesky, J. P., (2000), "Computer simulation of thread rolling Part 2: Study results," Fastener Technology International, No. 12, pp. 64-66.

[7] Edwards, C. M. and J. Halling, (1968), "An analysis of the plastic interaction of surface asperities and its relevance to the value of the coefficient of friction," Journal of Mechanical Engineering Sciences, Vol. 2, pp. 101-110.

[8] Goddard, J. and H. Wilman, (1962), "A theory of friction and wear during the abrasion of metals," Wear, Vol. 5, pp. 114-135.

[9] Haddow, J. B. and W. Johnson, (1961), "Indenting with pyramids - I. Theory," International Journal of Mechanical Sciences, Vol. 3, pp. 229-238.

[10] Haddow, J. B. and W. Johnson, (1961), "Indenting with pyramids - II. Experimental," International Journal of Mechanical Sciences, Vol. 4, pp. 1-13.

[11] Halling, J. and L. A. Mitchell, (1964), "Use of upper bound solutions for predicting the pressure for the plain extrusion of materials," Journal of Mechanical Engineering Science, Vol. 6, pp. 240-249.

[12] Hayama, M., (1972), "Estimation of torque in cold forming of internal thread," Bulletin of the Faculty of Engineering, Yokohama National University, Vol. 21, pp. 77-90.

[13] Henderer, W. E., and B. F. von Turkovich, (1974), "Theory of the cold forming tap," Annals of the CIRP, Vol. 23, pp. 51-52.

[14] Henderer, W. E., and B. F. von Turkovich, (1975), "Theory and experiments in tapping," Proceedings, North American Manufacturing Research Conference, Vol. 3, pp. 589-602.

[15] Hill, R. and S. J. Tupper, (1948), "A new theory of the plastic deformation in wire-drawing ," Journal of the Iron and Steel Institute, Vol. 159, pp. 353-359.

[16] Ivanov, V. and V. Kirov, (1997), "Rolling of internal threads: Part 1," Journal of Materials Processing Technology, Vol. 72, pp. 214-220.

[17] Ivanov, V., (1997), "Rolling of internal threads: Part 2," Journal of Materials Processing Technology, Vol. 72, pp. 221-225.

[18] Johnson, R. W. and G. W. Rowe, (1967-68), "Bulge formation in strip drawing with light reductions in area," Journal of Institution of Mechanical Engineers, Vol. 182, pp. 521-529.

[19] Rowe, G. W. and A. G. Wetton, (1965), "A simple correlation between deformation in some sliding wear and metal-working processes," Wear, Vol. 8, pp. 448-454.

[20] Rowe, G. W. and A. G. Wetton, (1969), "Theoretical considerations in the grinding of metals," Journal of Institute of Metals, Vol. 97, pp. 193-200.

[21] Zunkler, B., (1985), "Thread rolling torques with through rolling die heads and their relationship to the thread geometry and the properties of the workpiece material," Wire, Vol. 35, pp. 114-117.